

Hadron transverse momentum distributions and TMD studies

Jean-Francois Rajotte*

on behalf of the COMPASS Collaboration

Ludwig-Maximilians Universiteat, Fakultae fuer Physik,
D-80799 Munich, Germany

Abstract

Charged hadron differential distributions from muon-induced deep inelastic scattering, DIS, on a ${}^6\text{LiD}$ target are presented as function of the DIS variables x_{Bj} , Q^2 , W^2 and the hadron variables p_T and z . They can be used as benchmark to verify the reliability of theoretical model. The p_T^2 distributions are fitted with a Gaussian function at different kinematic intervals. With a Gaussian ansatz for the transverse momentum dependent parton distributions, TMDs, the intrinsic transverse momentum of the partons is extracted.

1 Introduction

Semi Inclusive Deep Inelastic Scattering (SIDIS) reactions provide much information about the structure of the nucleon and the hadronization of partons. Parton intrinsic transverse momentum affects the transverse momentum of the produced hadron. The kinematic variables of the produced hadron are shown in figure 1, where the transverse momentum is determined w.r.t. the virtual photon. The transverse momentum distributions from unpolarized scattering are often the first verification of the reliability of a theoretical model. The shape of the p_T^2 distributions depends on many effects, e.g. contribution from

*E-mail: jeanfrancois.rajotte@cern.ch

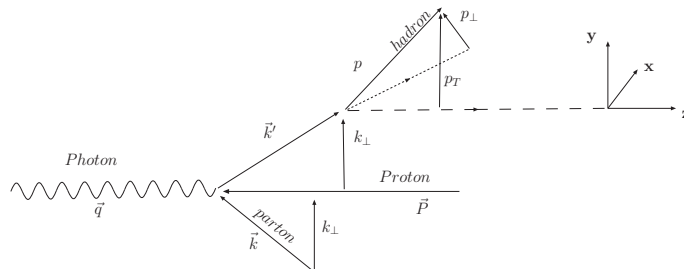


Figure 1: Kinematic variables of virtual photon interaction with a parton with intrinsic transverse momentum k_{\perp} and its hadronization. The transverse momentum of the observed hadron, p_T , is defined with respect to the virtual photon.

intrinsic transverse momentum k_{\perp} to the TMDs and transverse momentum of hadron p_{\perp} to the fragmentation functions (FFs) and gluon radiation. These effects depend on kinematic variables such as the Bjorken variable x_{Bj} , the invariant mass squared W^2 of the hadronic system, the negative 4-momentum squared Q^2 of the virtual photon and the virtual photon energy fraction z carried by the hadron. After integrating over the azimuthal angles, four variables are needed to describe the kinematics of the measured hadron: two inclusive (Q^2 , x_{Bj}) and two hadronic (p_T , z).

2 The COMPASS Experiment

The COMPASS experiment has been set up at the M2 muon beam line of the CERN SPS [1]. Polarized 160 GeV muons with an intensity of $2 \cdot 10^8 \mu/4.8 \text{ s}$ spill and a polarization of 80% are scattered off a polarized ${}^6\text{LiD}$ target. The target consists of two cells of opposite polarization which was reversed every 8 h. The unpolarized sample is therefore the combination of the data from the two cells. The COMPASS spectrometer is a large acceptance two-stage spectrometer which covers the kinematic range from quasi-real photo production to the DIS region. Both stages use hadron calorimeters and absorber walls for muon identification. The data presented here were taken during the year of 2004.

3 Hadron kinematic distributions

The charged hadron identification is kept as simple as possible. The particles coming out of the primary vertex are either identified as hadron or muons. From these hadrons, the selection requires that they create signals in the detector situated upstream and downstream of the first magnet. This ensures that the track momentum and charge are well defined by the bending of the magnetic field. The COMPASS ability to identify hadrons, with a RICH detector, was not used, but is intended for further analysis.

In order to correct for event losses caused by the non-uniform acceptance of the COMPASS spectrometer, a full Monte Carlo (MC) simulation has been performed. The events were generated with LEPTO, transported through the COMPASS detector simulation program COMGEANT and the reconstruction software CORAL. From this MC sample, 4-dimensional acceptance tables have been determined. Although very similar, positive and negative hadrons have different tables. The systematic error has been estimated to 5%. Only statistical errors are shown in the figures. In this analysis, the hadrons are separated into 23 intervals in Q^2 (from 1 to 10 GeV/c²) and x_{Bj} (from 0.004 to 0.12) further subdivided into 8 intervals in z (from 0.2 to 0.8).

4 Results

Hadron muoproduction has been studied for many years and the EMC experiment [5] covered a similar kinematic range as COMPASS. An interesting comparison with previous data is the ratio of positive and negative hadrons because the acceptance is canceled to a good approximation. The hadron multiplicity ratios are shown in figure 2. COMPASS results show clearly the z and x_{Bj} -dependence, where the fraction of positive hadrons increases with x_{Bj} (getting closer to the valence region) and z (more related to the struck parton). This agrees with the model of valence quarks where the positive quarks have a higher electric charge.

4.1 p_T^2 distributions

According to [4], the average over all p_T^2 should depend linearly on the center of mass energy squared, s . They have verified their prediction

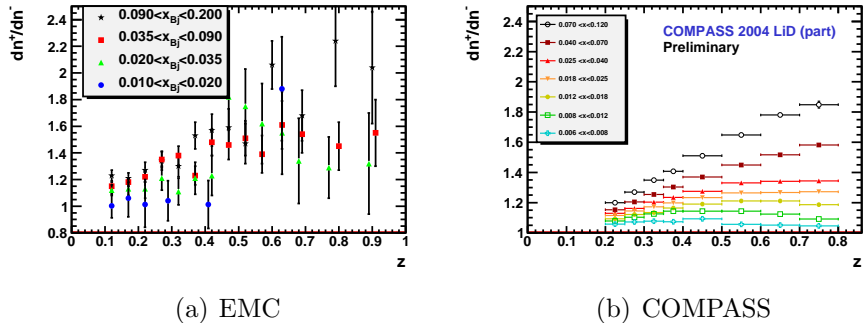


Figure 2: Charged hadron multiplicity ratios dn^+/dn^- as function of z for EMC [5] and COMPASS.

with results from three fixed target experiments: JLab, HERMES and COMPASS. The value used for COMPASS was not corrected for acceptance, the value is corrected here as shown in figure 3. The authors of [4] note that the average p_T^2 should depend linearly on W^2 rather than s . The dependence is shown in figure 4 which is more compatible with a linear dependence on W than on W^2 . The relation is not well established and, as mentioned in [4], the linear dependence on s for Drell-Yan which inspired their SIDIS prediction, could also be a linear dependence on \sqrt{s} . Figure 4 suggests the latter is more accurate.

4.2 Gaussian fit of the p_T^2 distributions and intrinsic transverse momentum

Using the Gaussian ansatz which assumes a Gaussian distribution of the intrinsic transverse momentum and of the transverse momentum acquired during fragmentation, the cross section is proportional to (cf. [2]):

$$\frac{d^4\sigma^{\mu P \rightarrow \mu+h+X}}{dx_{Bj}dQ^2dzdp_T^2} \propto \sum_q e_q^2 f_q(x_{Bj}) D_q^h(z) \frac{e^{-p_T^2/\langle p_T^2 \rangle}}{\pi \langle p_T^2 \rangle}, \quad (1)$$

where

$$\langle p_T^2 \rangle = \langle p_\perp^2 \rangle + z^2 \langle k_\perp^2 \rangle. \quad (2)$$

The functions $f_q(x_{Bj})$ and $D_q^h(z)$ are the usual (integrated) distribution and fragmentation functions, respectively. The distributions and

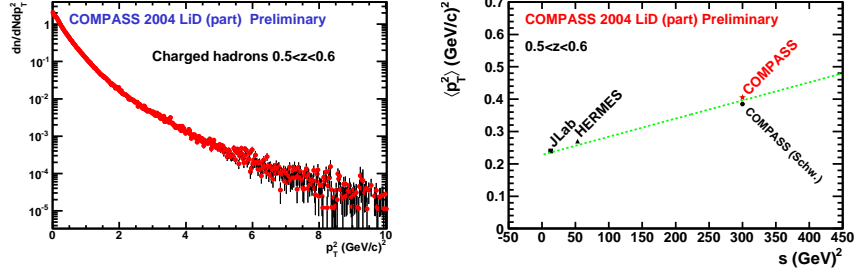


Figure 3: The left figure shows the differential p_T^2 distribution of hadrons with $0.5 < z < 0.6$. It is used to determine the corrected COMPASS averaged over all p_T^2 . This value is to correct the figure on the right from [4], where three experiments show the s -dependence of the average p_T^2 . The red star COMPASS point is the value from this analysis, the black dot, COMPASS (Schw.), is the value inferred by [4] from data uncorrected for acceptance.

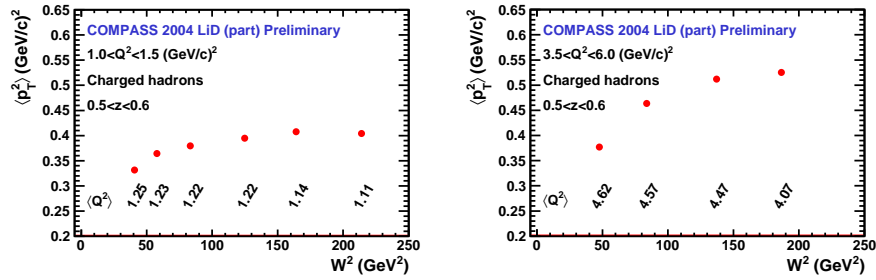


Figure 4: Charged hadron average over all p_T^2 vs W^2 . Note that contrary to all the following figures of this article, $\langle p_T^2 \rangle$ defines a standard average over all p_T^2 .

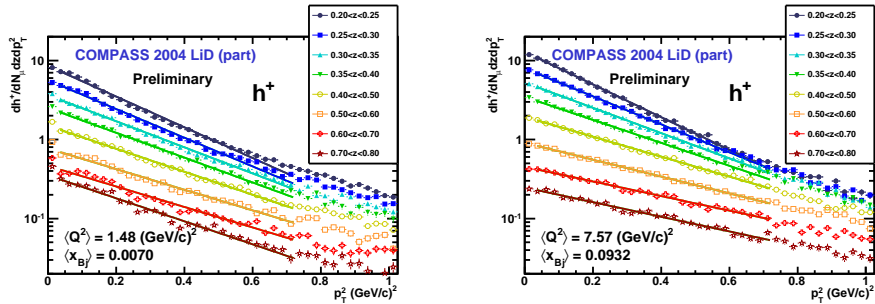


Figure 5: p_T^2 distributions fitted by a Gaussian for $(1 < Q^2 < 1.5 \text{ (GeV/c)}^2, 0.006 < x_{Bj} < 0.008)$ and $(6 < Q^2 < 10 \text{ (GeV/c)}^2, 0.07 < x_{Bj} < 0.12)$ subdivided into 8 z intervals.

fits for two (Q^2, x_{Bj}) intervals and for all z intervals are shown in figure 5. The fit is performed on the low p_T interval $[0.1, 0.85] \text{ GeV/c}$ in order to stay away from pQCD effect. The fitted $\langle p_T^2 \rangle$ as function of x_{Bj} are shown in figure 6 for low and high z . A similar behavior was already observed by HERMES in [6] for the average p_T (not from a fit but from a standard average). It is interesting to compare the average p_T^2 from the previous section (figure 4) with the fitted $\langle p_T^2 \rangle$ for the middle z shown in figure 7. Contrary to the average over all p_T^2 , there is no clear W^2 -dependence of the fitted $\langle p_T^2 \rangle$ (for $0.1 < p_T < 0.85 \text{ GeV/c}$) which is suppose to be unaffected by pQCD.

The z^2 -dependence of the fitted $\langle p_T^2 \rangle$ is of particular interest because of its relation to the intrinsic transverse momentum through equation (2). The fitted $\langle p_T^2 \rangle$ for different z^2 for two (Q^2, x_{Bj}) intervals are shown in figure 8. The relation between $\langle p_T^2 \rangle$ and z^2 is certainly not linear as in equation (2). If a z -dependence of the transverse momentum acquired during fragmentation, p_\perp , is added such that

$$\langle p_T^2 \rangle = z^\alpha (1 - z)^\beta \langle p_\perp^2 \rangle + z^2 \langle k_\perp^2 \rangle, \quad (3)$$

where $\alpha = 0.5$ and $\beta = 1.5$, the relation can be nicely fitted as shown in figure 8. From this fit, the intrinsic momentum, $\langle k_\perp^2 \rangle$, for various (Q^2, x_{Bj}) intervals can be extracted. The extracted $\langle k_\perp^2 \rangle$ as function of Q^2 are shown in figure 9 and as function of x_{Bj} , comparing results from positive and negative hadrons, are shown in 10.

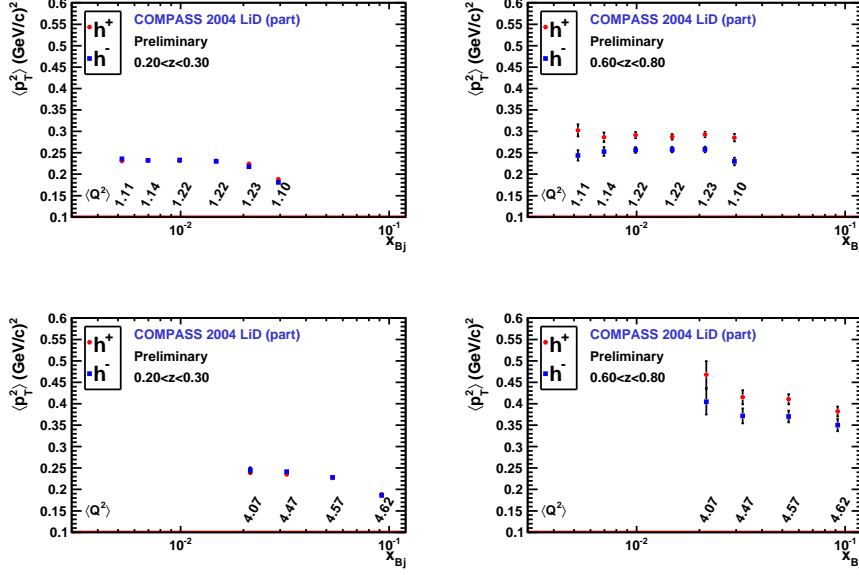


Figure 6: Fitted $\langle p_T^2 \rangle$ vs x_{Bj} for different Q^2 intervals for low (left column) and high (right column) z . In the present figure, the $\langle p_T^2 \rangle$ results from a fit over $p_T < 0.85$ GeV/c.

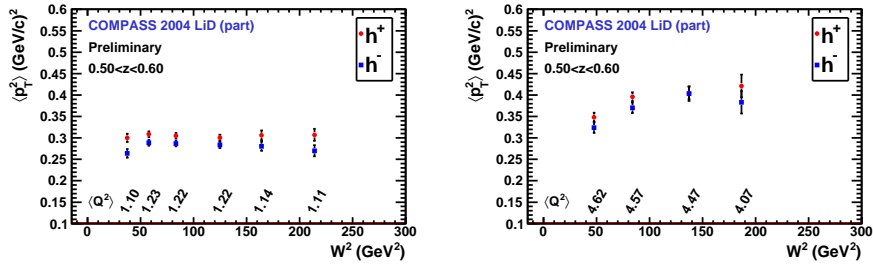


Figure 7: Fitted $\langle p_T^2 \rangle$ vs W^2 at medium z ($[0.5, 0.6]$) for different Q^2 intervals. This is to be compared with figure 4 where the average over all p_T^2 is plotted. In the present figure, the $\langle p_T^2 \rangle$ results from a fit over $p_T < 0.85$ GeV/c.

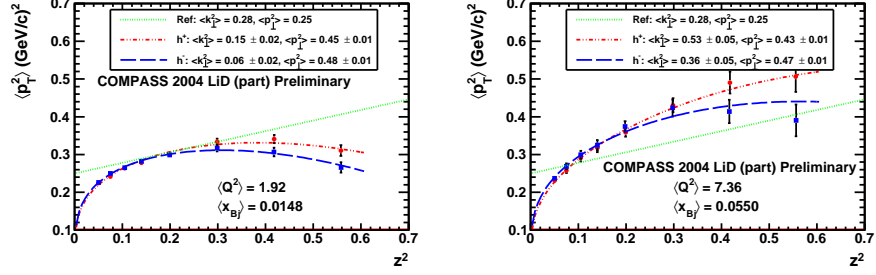


Figure 8: Fitted $\langle p_T^2 \rangle$ vs z^2 for two (Q^2, x_{Bj}) intervals. The fit function is given by equation (3). The dotted green line is the result of a fit, performed by [3], to data from many experiments. In the present figure, the $\langle p_T^2 \rangle$ results from a fit over $p_T < 0.85$ GeV/c.

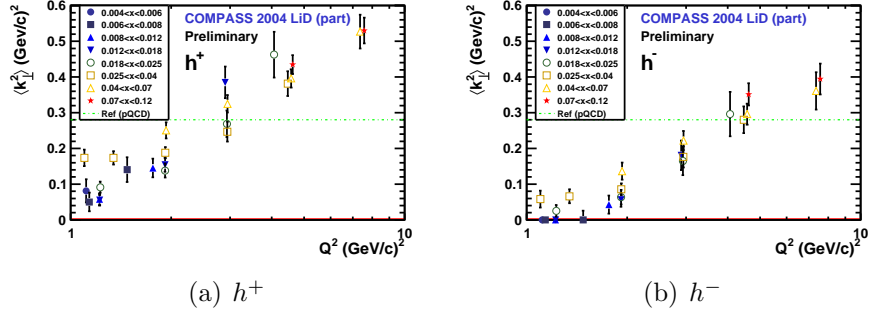


Figure 9: Extracted $\langle k_{\perp}^2 \rangle$ vs Q^2 for various x_{Bj} intervals. The dotted green line is the result of a fit, performed by [3], to data from many experiments.

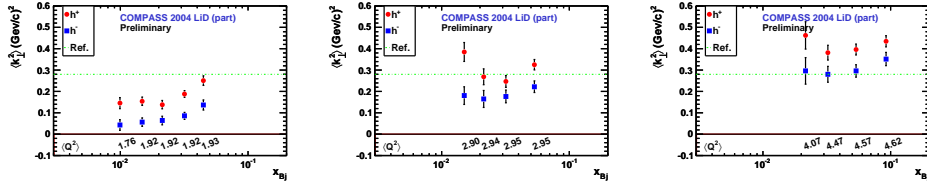


Figure 10: Extracted $\langle k_{\perp}^2 \rangle$ vs x_{Bj} for positive and negative hadron comparison. The dotted green line is the result of a fit, performed by [3], to data from many experiments.

5 Conclusion

The differential p_T^2 distributions of charged hadrons produced by muons scattered off a ${}^6\text{LiD}$ target have been determined for various kinematic intervals. The low p_T^2 have been fitted with a Gaussian at different z such that the intrinsic transverse momentum could be extracted in the framework of the Gaussian ansatz. The non linear relation between the fitted $\langle p_T^2 \rangle$ and z^2 have been reproduced by adding a z -dependence of the transverse momentum acquired during fragmentation. The extracted $\langle k_\perp^2 \rangle$ shows a clear dependence on Q^2 and a possible dependence on x_{Bj} , although less conspicuous for higher Q^2 , where the framework is more reliable. Also, $\langle k_\perp^2 \rangle$ is systematically higher for positive hadrons compared to negative hadrons. This suggests a flavor dependence of the intrinsic transverse momentum. This behavior could be further investigated using COMPASS ability to identify hadrons; kaon identification could provide access to characteristics of the strange quark TMDs.

Acknowledgment

I would like to thank Dr. Alessandro Bacchetta for his helpful comments.

References

- [1] Abbon, P. and others, Nucl. Instrum. Meth. **A577**, (2007) 455-518
- [2] Anselmino, M. and others, Phys. Rev. **D71**, (2005) 074006
- [3] Anselmino, M. and Boglione, M. and Prokudin, A. and Turk, C., Eur. Phys. J. **A31**, (2007) 373-381
- [4] Schweitzer, P. and Teckentrup, T. and Metz, A., Phys. Rev. **D81**, (2010) 094019
- [5] Ashman, J. and others, Z. Phys. **C52**, (1991) 361-388
- [6] Jgoun, Anton on behalf of the HERMES collaboration, Talk given at 36th Rencontres de Moriond on QCD and Hadronic Interactions, (2001)